Proceedings of the 11th International Coral Reef Symposium, Ft. Lauderdale, Florida, 7-11 July 2008
Session number 17

A pan-sharpening method for satellite image-based coral reef monitoring with higher accuracy

H. Hanaizumi[1], M. Akiba[1], H. Yamano[2], T. Matsunaga[2]

1) Hosei University, Faculty of Computer and Information Sciences, 3-7-2 Kajino-cho, Koganei, Tokyo 184-8584, Japan
2) National Institute of Environmental Studies, Center for Global environmental Research, 16-2 Onogawa, Tsukuba, Ibaraki 305-8506, Japan

Abstract. A pan-sharpening method for enhancing satellite imagery is proposed as the first step for building a relatively high accuracy and low cost approach for image-based analyses of coral reefs. To achieve this objective, a low spatial resolution multi-spectral image was first spatially resampled (increasing the number of pixels) and co-registered onto a higher resolution panchromatic image. Based on multiple regression analysis, brightness information of the resampled multi-spectral image was replaced with that of the panchromatic image so that all spectral density scatter-diagrams exhibit linear characteristics with slopes equal to one and *y*-intercepts equal to zero. The method was characterized by its simplicity and faithfulness in preserving spectral (i.e., color) information. Since the resampled multi-spectral pixels were independently modified by the densities of the panchromatic pixels, all information in the panchromatic image was transferred to the resulting pan-sharpened image, thus producing lossless pan-sharpening. As a demonstration, the method was applied to FORMOSAT-2 data acquired on 31 January 2007 at Ishigaki Island, Ryukyu Islands, Japan.

Key words: Lossless pan-sharpening, panchromatic, multi-spectral, spatial resolution.

Introduction

A method for observing global changes in coral reef status is required. Remote sensing is an effective tool to map and detect broad-scale changes of coral reefs. The effectiveness of the mapping and detection using remote sensing depends on the spatial resolution of the imagery, where higher spatial resolution generally result in higher accuracy (Mumby and Edwards 2002; Andréfouët et al. 2002, 2003; Yamano and Tamura 2004). However, high-resolution satellite images are typically costly to acquire and process, which often discourages their use.

One solution to the cost issue is to introduce a pan-sharpening method to transform coarser spatial resolution satellite images into higher spatial resolutions (Nishii et al. 1996; Liu 2000). This approach has the potential to provide high-spatial resolution data at a lower cost than the direct purchase of high resolution multi-spectral imagery. Pan-sharpening is a data fusion method whereby the spatial resolution of a multi-spectral image is improved by injecting information extracted from a higher resolution panchromatic band. There have been many algorithms proposed for this type of data fusion. Recently, a public contest for pan-sharpening algorithms was performed (Alparone et al. 2007). Eight algorithms were evaluated in this contest and the GLP-CBD (Aiazzi et al. 2002, 2006) and AWLP (Otazu et al. 2005) algorithms were ultimately ranked as the best. Both algorithms use multi-resolution analysis (MRA) to achieve spatial enhancement and were derived directly from the values measured by the sensor. The algorithms also use a normalization process when transforming the multi-spectral pixel values using the panchromatic information to avoid spectral distortion

For effective image analysis, pan-sharpening methods should preserve spectral information throughout the image, including both land and water areas, and reduce errors associated with noise such as breaking waves. Since complicated processing itself may cause unpredictable noise, the pan-sharpening process approach should also ideally be simple and predictable. We propose a simple pan-sharpening method based on a multiple regression analysis. In the method, original multi-spectral images are spatially resampled (increasing number of pixels) and then modified so that scatter diagrams between pan-sharpened image and the resampled original image for all spectral bands exhibit linear relationships with slopes equal to one and *y*-intercepts equal to zero.

Material and Methods

A set of FORMOSAT-2 (Liu 2006) images acquired on 31 January 2007 at Ishigaki Island, Ryukyuu-Islands, Japan were used to demonstrate the proposed

pan-sharpening method. FORMOSAT-2 provides a total of four visible-near infrared multi-spectral bands at 8 x 8 m^2 spatial resolution and a panchromatic band at 2 x 2 m^2 spatial resolution. The panchromatic band covers the same equivalent spectral range as the four visible-near infrared bands.

Pan-Sharpening Model

In the proposed method, pan-sharpening is accomplished by replacing brightness information estimated from the original lower resolution multi-spectral (MS) bands with values derived from the higher spatial resolution panchromatic band. This process is performed while preserving the spectral information for subsequent image classification and analysis. Figure 1 illustrates how pixels for a single original MS pixel correspond with the 16 PAN pixels, and the resulting 16 pan-sharpened MS pixels. As shown in Fig. 1, the spectral reflectance values of the original MS are written as r (red), g (green), b (blue) and n (near infrared), and the corresponding panchromatic reflectance values are P_1 .. P_{16}. We regard the pan-sharpening problem as calculating the values r_i^P, g_i^P, b_i^P, n_i^P (i = 1 .. 16) as a function of a brightness estimator y, which is formulated as

$$y = f(r, g, b, n, P_1, \cdots, P_{16}). \tag{1}$$

In an early formulation of this algorithm (Gillespie et al. 1987), y was calculated simply as

$$y = (r + g + b)/3. \tag{2}$$

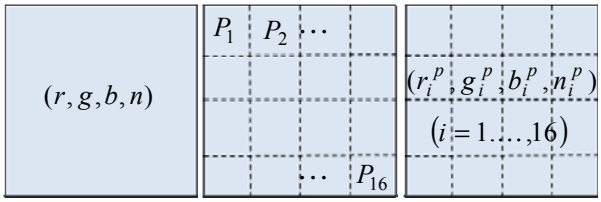

Figure 1: (a) Original MS pixel, (b) PAN pixels, and (c) pan-sharpened MS pixels.

Eq. (2) indicates that the brightness y is estimated by using just the lower resolution image, where the sum of r, g and b is a rough approximation of overall brightness. Liu used a more sophisticated function (Liu 2000) with y calculated as

$$y = \frac{1}{N}\sum_{i=1}^{N} P_i, \tag{3}$$

where N is the number of high resolution pixels corresponding to the lower resolution pixel. Liu's estimator was thus calculated using only the high resolution image. Once the estimator is obtained in the Gillespie et al. (1987) or Liu (2000) methods, the pan-sharpened values r_i^P, g_i^P, b_i^P, n_i^P (i = 1 .. 16) are calculated as

$$\left.\begin{aligned} r_i^p &= \frac{r}{y} P_i \\ g_i^p &= \frac{g}{y} P_i \\ b_i^p &= \frac{b}{y} P_i \end{aligned}\right\} (i = 1, \cdots, 16). \tag{4}$$

Since Liu's method is a form of a high pass filter, it works particularly well in photo interpretation. Both of the above methods, however, do not exactly preserve the spectral characteristics of the original multi-spectral image. This is evident when observing the scatter diagram of the original low resolution image and resulting pan-sharpened image does not have a linear relationship.

The proposed method is designed so that the pan-sharpened versus original density scatter diagram gives a perfectly linear relation with slope equal to one and a zero y-intercept. The method is a generalized algorithm that is equally applicable to both land and water applications. In this method we calculate the brightness estimator y as

$$y = a_0 r + a_1 g + a_2 b + a_3 n + a_4. \tag{5}$$

This model is derived from the fact that the panchromatic band covers the same spectral range as the visible (red, green, blue) and near infrared bands combined. Since the near infrared band reflectance is high in land (non-water) areas and almost zero in water areas, two separate versions of the model are utilized to independently represent the land and water areas respectively.

In the proposed method, each original multi-spectral pixel is first resampled into N pixels (N = 16 for FORMOSAT-2) so that resampled image has the same number of pixels as the panchromatic. All of the N pixels are initially assigned the same reflectance values as the original pixel

$$\left.\begin{aligned} r_i^e &= r \\ g_i^e &= g \\ b_i^e &= b \\ n_i^e &= n \end{aligned}\right\} (i = 1, \ldots, 16). \tag{6}$$

For the resampled image, Eq.(5) is rewritten as

$$y^e = a_0 r^e + a_1 g^e + a_2 b^e + a_3 n^e + a_4, \tag{7}$$

where y^e means brightness component of expanded pixel (i.e., resampled pixel). Using Eq.(7), the pan-sharpened reflectance values are calculated as

$$\left.\begin{aligned} r_j^p &= \frac{r_j^e}{y_j^e} P_j \\ g_j^p &= \frac{g_j^e}{y_j^e} P_j \\ b_j^p &= \frac{b_j^e}{y_j^e} P_j \end{aligned}\right\} (j = 1, \ldots, M), \qquad (8)$$

where M is the total number of pixels in the panchromatic image. Thus, the pan-sharpening problem is reduced to determining the coefficients a_0, a_1, a_2 and a_4 in Eq.(7). It is evident from Eq.(8) that when y_j^e equals to P_j the pan-sharpened pixel values are statistically the same as the original.

We use a multiple regression analysis to determine the coefficients as

$$P_j = a_0 r_j^e + a_1 g_j^e + a_2 b_j^e + a_3 n_j^e + a_4 \qquad (9)$$
$$(j = 1, \ldots, M).$$

Eq.(9) is rewritten as

$$\begin{bmatrix} P_1 \\ P_2 \\ \vdots \\ P_M \end{bmatrix} = \begin{bmatrix} r_1^e & g_1^e & b_1^e & n_1^e & 1 \\ r_2^e & g_2^e & b_2^e & n_2^e & 1 \\ \vdots & \vdots & \vdots & \vdots & \vdots \\ r_M^e & g_M^e & b_M^e & n_M^e & 1 \end{bmatrix} \begin{bmatrix} a_0 \\ a_1 \\ a_2 \\ a_3 \\ a_4 \end{bmatrix}, \qquad (10)$$

or in matrix format as

$$\mathbf{P} = \mathbf{XA}. \qquad (11)$$

The coefficient vector **A** is obtained by using a generalized inverse solution

$$\mathbf{A} = (\mathbf{X}'\mathbf{X})^{-1}\mathbf{X}'\mathbf{P}, \qquad (12)$$

where **X**‘ is the transpose matrix of **X** and $\mathbf{X}^{-1}$ is the inverse matrix of **X**. The pan-sharpened multi-spectral reflectance values are obtained by solving Eqs.(7), (8) and (12).

Spatial Co-Registration

The MS and PAN sensors on FORMOSAT-2 are physically separated, which produces a complex discrepancy in spatial registration between the two sensors. In order to remove this discrepancy, a spatial co-registration process (Hanaizumi et al. 1994) was applied to the FORMOSAT-2 imagery before implementing the pan-sharpening procedure. The co-registration process consisted of automated searching for common points in the MS and PAN bands, Delaunay triangulation using the identified points, and piece-wise affine transformation for removing the discrepancy and performing the co-registration. Since all of the MS bands are already co-registered, the co-registration process was simplified by first generating a single pseudo image by adding together the reflectance values from the individual *r*, *g*, *b* and *n* images. Analysis was then performed by co-registering the pseudo image with the PAN image. Approximately 1000 points were automatically identified as co-occurring in the pseudo and PAN images. Delaunay triangulation was used to generate a surface network from these points, and piece-wise affine transformation was then used to remove the discrepancy. In this approach, only the convex areas of the Delaunay triangulation were included in the co-registration process and subsequently utilized in the pan-sharpening model.

Results and discussion

The co-registration and pan-sharpening methods were applied to the FORMOSAT-2 imagery of the northern area of Ishigaki Island. The original imagery measured 4443 x 5359 pixels for the MS bands and 17321 x 19679 pixels in the PAN image. For the pan-sharpening model, all four MS bands (*r*,*g*,*b*,*n*) were used over land (non-water) and only the three visible bands (*r*,*g*,*b*) were used over water, which includes the coral reef areas of interest. Figure 2 shows the pan-sharpening results for a 3000 x 3000 pixel subset of the overall image.

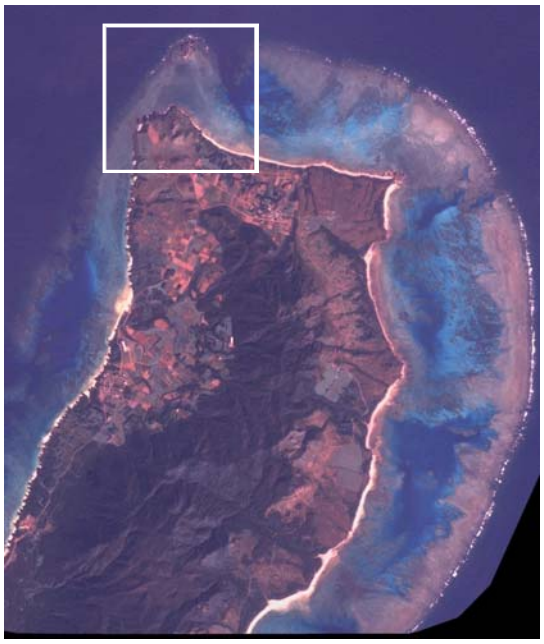

Figure 2: Pan-sharpening output for image subset, with focus area highlighted in white.

Figure 3 compares the pan-sharpening output with the original resampled image for the 800 x 800 pixel focus area indicated in Figure 2. It can be qualitatively observed that the pan-sharpened image preserves information from both the MS and PAN bands. This is because the pan-sharpening method modifies the MS pixel values using information from all bands.

In order to quantitatively evaluate the performance of the pan-sharpening model with respect to preserving spectral information, scatter diagrams were produced comparing the original resampled MS pixel values with the resulting pan-sharpened values. Ideally, this should be a linear 1:1 relationship, with a slope of one and a zero *y*-intercept. Figure 4 shows the reflectance scatter diagrams for the *r*, *g* and *b* spectral bands. In these diagrams, the *x*-axis indicates pixel values from the original MS image, and the *y*-axis is the pixel values after pan-sharpening. Further, the intensity (i.e., darkness) of each dot is proportional to the logarithmic frequency of pixels with that specific value. The red lines in these diagrams indicate the ideal 1:1 relationship. We can see that all scatter diagrams produce linear shapes closely approximating the 1:1 line. This indicates that the spectral information is preserved and that we have effectively obtained a higher spatial resolution color image of the coral reefs from the lower resolution original.

Conclusions

A pan-sharpening method was proposed which incorporates the panchromatic information without distorting the original spectral information. Application to coral reef imagery produced a visual improvement. The pan-sharpening was performed pixel-by-pixel, replacing brightness components of each lower spatial resolution MS band with higher spatial resolution values derived from the MS and PAN bands. It was also quantitatively shown that the resulting pan-sharpened image preserved the spectral (i.e., color) content of the original image. The multiple regression analysis used for this estimation is regarded as a type of density normalization between

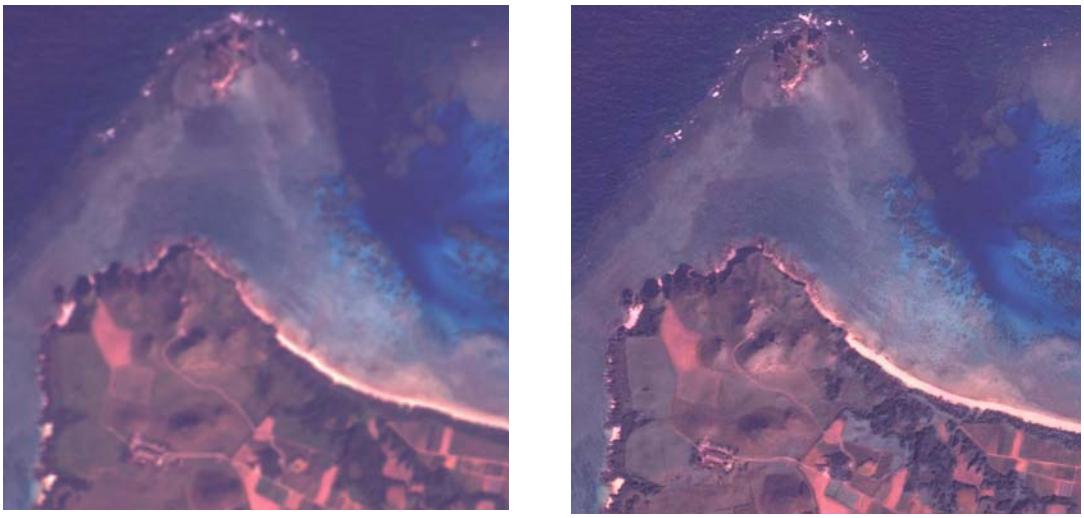

(a) MS original color image. (b) Pan-sharpened image.

Figure 3: Comparison of pan-sharpening results with the resampled original image for a 800 x 800 pixel focus area.

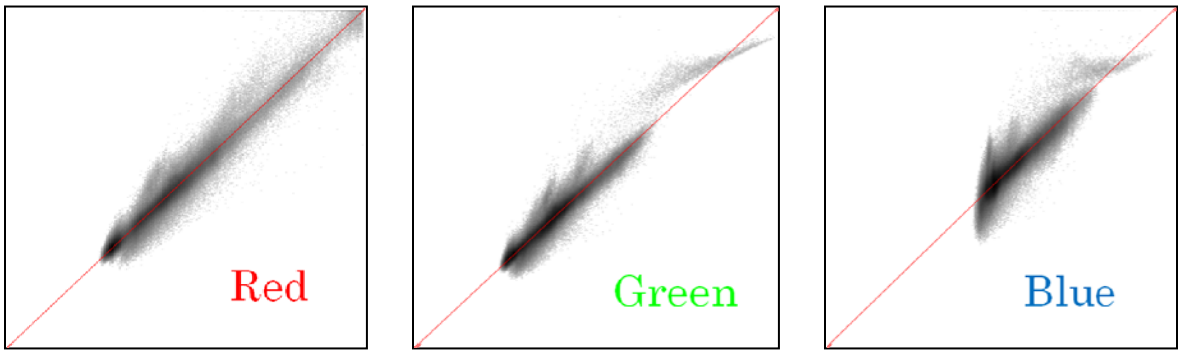

(a) Red band. (b) Green band . (c) Blue band.

Figure 4: Density scatter diagrams between the pan-sharpened result (y-axis) and the original MS imgary (x-axis).

the multi-spectral bands and the panchromatic image. The model is applied over water using just the three visible MS bands, and over land using all four MS bands. By incorporating the higher resolution panchromatic information, the model also adds spatial information not present in the original lower resolution image.

The proposed method was successfully applied to FORMOSAT-2 data of Ishigaki Island, Japan. The spatial resolution of the MS bands was improved from 8 x 8 m to 2 x 2 m by implementing the pan-sharpening model. Spectral preservation performance was evaluated using scatter diagrams, which indicated results approximating the desired 1:1 relationship and thus confirmed effective performance of the model.

The authors next plan on using pan-sharpening method to monitor temporal changes in coral reefs using satellite remote sensing imagery. The development of appropriate change detection methods using this imagery is a subject of future study.

References

Aiazzi B, et al. (2002) Context-driven fusion of high spatial and spectral resolution data based on oversampled multiresolution analysis. IEEE Trans GRS-40-10:2300-2312

Aiazzi B, et al. (2006) <TF-tailored mutiscale fusion of high-resolution MS and Pan imagery. Photogramm. Eng Remote Sens 72-5:591-596

Alparone L, et al. (2007) Comparison of Pansharpening Algorithms: Outcome of the 2006 GRS-S Data-Fusion Contest. IEEE Trans. GRS-45-10:3012-3021

Andréfouët S, Berklemans R, Odrizola L, Done T, Oliver J, Muller-Karger F (2002) Choosing the appropriate spatial resolution for monitoring coral bleaching events using remote sensing. Coral Reefs 21: 147-154

Andréfouët S, Kramer P, Torres-Pulliza D, Joyce KE, Hochberg EJ, Garza-Perez R, Mumby PJ, Riegl B, Yamano H, White WH, Zubia M, Brock JC, Phinn SR, Naseer A, Hatcher BG, Muller-Karger F (2003) Multi-site evaluation of IKONOS data for classification of tropical coral reef environments. Remote Sens Environ 88: 128-143

Brown BE (1997) Coral bleaching: Causes and consequences. Coral Reefs 16:129-138

Gillespie AR et al. (1987) Color enhancement of highly correlated images—II. Channel ratio and 'chromaticity' transformation techniques. Remote Sens Environ 22: 343-365

Glynn PW (1993) Coral reef bleaching: Ecological perspectives. Coral Reefs 12:1-17

Hanaizumi H et al. (1994) An automated method for making mosaic out of NOAA/AVHRR images for global monitoring. Proc IGARSS'94 3: 1808-1810

Hoegh-Guldberg O (1999) Climete change, coral bleaching and the future of the world's coral reefs, Mar Freshw Res 50:839-866

Liu CC (2006) Processing of FORMOSAT-2 Daily Revisit Imagery for Site Surveillance. IEEE Trans. GRS-44-11: 3206-3214

Liu JG (2000) Smoothing Filter-based Intensity Modulation: a spectral preserve image fusion technique for improving spatial details. Int J Remote Sens. 21-18:3461-3472

Mumby PJ, Edwards AJ (2002) Mapping marine environments with IKONOS imagery: enhanced spatial resolution can deliver greater thematic accuracy. Remote Sens Environ 82: 248-257

Nishii R, Kusanobu S, Tanaka S (1996) Enhancement of Low Spatial resolution Image Based on High resolution Bands. IEEE Trans. GRS-34-5:1151-1158

Otazu X et al. (2005) Introduction of sensor spectral response into image fusion methods: Application to wavelet-based methods. IEEE Trans. GRS-43-10:2376-2385

Wilkinson CR (2000) Status of coral reefs of the world: 2000. Queensland: Australian Institute of Marine Science

Yamano H, Tamura M (2004) Detection limits of coral reef bleaching by satellite remote sensing: Simulation and data analysis. Remote Sens Environ 90: 86-103